Journal of Neurogenetics (2005); 19(3-4):143-54

QUANTITATIVE ANALYSIS OF MICROGLIAL CELLS IN THE DEGENERATING CEREBELLUM OF THE STAGGERER (RORA$^{sg/sg}$) MUTANT MOUSE.

NATHALIE JOURNIAC, MOHAMED DOULAZMI, FABRICE PAJAK, JEAN MARIANI and BEATRICE VERNET-DER GARABEDIAN*

UMR 7102 Neurobiologie des Processus Adaptatifs, CNRS and Université P.&M. Curie, Equipe Développement et Vieillissement du Système Nerveux , Boîte 14, 9 quai Saint Bernard, 75 005, Paris, France

* Corresponding author. Fax : (33 1) 44 27 22 80; email: bvernet@snv.jussieu.fr

Abbreviated title: Microglia in Rora$^{sg/sg}$ Cerebellum

Summary:

Elevated levels of pro-inflammatory cytokines such as IL-1ß and IL-6 have been detected in the cerebellum of *Rora*$^{sg/sg}$ mice in which a neurodegenerative process occurs during the first postnatal month. This suggests the existence of a microglial reaction in the context of an inflammatory process that would be triggered by the massive neuronal loss. To test this hypothesis, we qualitatively and quantitatively studied the microglial cell population using lectin and nucleosidic diphosphatase labeling of the cerebellum of 30 day-old mice. The massive neuronal loss induces a 11.7 fold smaller size of the *Rora*$^{sg/sg}$ cerebellum compared to the wild-type. We showed that the *Rora*$^{sg/sg}$ microglia population is exclusively composed of cells displaying the characteristic morphology of activated cells, with enlarged strongly stained cell bodies and few thick processes, in contrast to microglial cells in the wild-type. The density of microglia is 2.7 fold higher in *Rora*$^{sg/sg}$ than in wild-type mice (22444 ± 5011 cells/mm^3 versus 8158 ± 1584 cells/mm^3), although the absolute number is 4-fold smaller. These results show that neurodegeneration in the *Rora*$^{sg/sg}$ cerebellum leads to persistance of microglial activation while in wild-type it disappears around P10.

Keywords : *Rora* , CNS, neurodegeneration, inflammation.

INTRODUCTION

The ataxic homozygous *staggerer* (*Rora*$^{sg/sg}$) mutant mouse was originally described as a cerebellar mutant that was widely used to highlight both the establishment of cerebellar connectivity and neurodegenerative processes. However, nothing is known about microglial cell reaction to the perinatal massive neuronal loss in the Rora$^{sg/sg}$ cerebellum. The staggerer mutation is an autosomal semi-dominant mutation located on chromosome 9. The gene encoding the Retinoic acid receptor-related Orphan Receptor (Rora) has been identified as the site of the mutation. Rora is a member of the superfamily of nuclear receptors. The staggerer mutation is a 122 bp deletion in the ligand-binding domain of Rora (Hamilton et al., 1996) that leads to loss of function. It is expressed in a wide variety of tissues, explaining why Rora$^{sg/sg}$ mice display numerous phenotypes besides their ataxia, including immune abnormalities (Jarvis et al., 2002). In the central nervous system (CNS), expression of Rora has been detected in neurons of the cerebellum, inferior olive, hippocampus, thalamus, cortex, hypothalamus, retinal ganglion cells and olfactory bulb (Matsui et al., 1995; Monnier et al., 1999). Expression of mutated Rora gene in Purkinje cells lead to a deficit of 82% of these cells in the *Rora*$^{sg/sg}$ adult cerebellum (Doulazmi et al., 2001). Target–related cell death affects all the granule cells and 60% of the olivary neurons by the end of the first post-natal month (Sidman et al., 1962; Herrup & Mullen, 1979; Shojaeian et al., 1994). The absence of granule cells, the most numerous neurons in the cerebellum, leads to a cerebellar atrophy often described as severe. Consequences for the cerebellar volume of adult homozygous staggerer have never been quantified. This massive neuronal loss is likely associated with an inflammatory reaction. Indeed astrogliosis, has been described 20 years ago after biochemical and morphological studies (Seyfried & Yu, 1984; Levine et al., 1986). More recently, we have shown elevated levels of IL-1ß and of IL-6 in the cerebellum of one month-old *Rora*$^{sg/sg}$ mice compared to the wild-type (Lemaigre-Dubreuil et al., 1996; Vernet-der Garabedian et al., 1998). These two cytokines, mainly produced by activated microglial cells in the CNS, are key mediators in initiating, amplifying and regulating inflammation that develops in reaction to situations compromising the nervous tissue integrity (Basu et al., 2004). Microglia are thus key effector cells in the inflammatory process. Microglial activation is a characteristic of acute CNS injury as well as neurodegenerative and inflammatory diseases (Kreutzberg, 1996).

Whether an inflammatory reaction develops in the *Rora*$^{sg/sg}$ cerebellum in response to the massive loss of cerebellar neurons is not completely established. One of the most conspicuous features of microglia activation is a spectacular morphological change. Activated microglial cells have a round or amoeboid shape, with a swollen cell body and a few short processes; in contrast, resting microglial cells display small cell bodies and long thin branched processes (Wu et al., 1992). We have therefore evaluated the microglial population in terms of their morphology and number in the cerebellum of *Rora*$^{sg/sg}$ mice.

MATERIALS AND METHODS

Animals

Thirty-day old homozygous *Rora*$^{sg/sg}$ (n=3) and age-matched wild-type (n=3) mice were used in this study. The *staggerer* mutation was bred on C57BL/6J background. Homozygous *Rora*$^{sg/sg}$ mutants were identified by their ataxic behavior around postnatal day 15 in litters from *Rora*$^{sg/+}$ x *Rora*$^{sg/+}$ matings. Wild-type (*Rora*$^{+/+}$) animals from the same litter were identified using PCR performed on tail DNA extract as previously described (Doulazmi et al., 1999). All animals used in strict compliance with the relevant welfare guidelines adopted by the European Community.

Microglia labeling

Different methods are available to visualize microglia including silver staining, immunohistochemistry, lectin histochemistry and nucleosidic diphosphatase (NDPase) detection. Silver staining is a rather nonspecific method labeling not only microglia, but also oligodendrocytes. Immunohistochemistry usually gives stronger labeling of amoeboid than ramified microglia or does not stain ramified microglia at all. Although lectin and NDPase label also endothelial cells, these two methods were used for microglial staining in the present study because they have the same specificity and they reliably label both reactive and resting microglia. Lectin labeling with Griffonia simplicifolia B4 (GS-B4) was used to count microglial cells and detection of nucleosidic diphosphatase (NDPase) activity for qualitative analysis.

Lectin binding : mice were anesthetized by an intraperitoneal injection of 3,5% of chloralhydrate (0.1ml/g weight) and transcardially perfused with 300 ml of 0.1 M phosphate buffer saline pH 7 .4 containing 4% paraformaldehyde (PBS-PFA). Brains were dissected out, post-fixed for 24h in PBS-PFA and cryoprotected in 30% sucrose in PBS overnight. The entire cerebellum was cut in serial sections of 18 µm, mounted on gelatinized slides, and air-dried. Lectin labelling was carried out on all sections as previously described (Streit & Kreutzberg, 1987) with minor modifications. Briefly, sections were washed twice in PBS, then incubated with 30 µg/ml of GS-B4 conjugated to horseradish peroxydase (HRP) in 0.1% Triton X-100 for 24h at 4°C. The GS-B4 binding was detected by the HRP reaction using diaminobenzidine as chromogen. As a negative control, GS-B4 was omitted. Slides were then dehydrated in graded ethanol, cleared in toluene and mounted in Eukitt.

NDPase activity : the detection of NDPase activity was carried out as previously described (Murabe & Sano, 1982). Briefly, mice were anesthetized as described and transcardiacally perfused with 4% of paraformaldehyde diluted in 0.1M cacodylate buffer pH 7.2, containing 8% of saccharose and 5% of dimethylsulfoxide (DMSO). Brains were dissected out, post-fixed with the same fixative overnight at 4°C and were rinsed in the same buffer. A half-brain was then cut in 30 µm sagital sections and kept in 8% saccharose in 0.2M Tris–maleate buffer pH 7.2. Sections were incubated with 2 mM of 5'-diphosphate-uridine in 80 mM Tris-maleate buffer pH 7.2 containing 0.12% of lead-citrate, 5 mM of manganese chloride and 1% of DMSO for 30 min at 37°C. Incubating sections in 2% ammonium sulfide produced a reaction product, a brown colored precipitate.

Microglial cell count

Cerebellar microglial cell numbers in Rora$^{sg/sg}$ and wild-type mice were counted on GS-B4 stained sections from three animals in each group. We used lectin labeling because of the reliability and robustness of this method. Estimation of cell density was performed as previously described (Vela et al., 1995). The cerebellar surface of every section was drawn and measured using an image analysis system (Saga Biocom-France). The cerebellar volume was calculated as the product of the total surface of sections by the thickness. Microglial cells were counted on twelve sections per animals at the interval of 300 µm. All labeled microglial cells with a cytoplasmic shape found in the cerebellar surface were counted, excluding the intravascular cells. The density was calculated for each examined section as the number of counted cells divided by the measured surface. For each non-counted section, the density was extrapolated by considering that, between two counted sections, the density varied linearly with the raw of intermediate section. The sum of all sections gave the total number of microglial cells per cerebellum. We chose to use this traditional cell counting method instead of more recently developed stereological techniques (Wirenfeldt et al., 2003), so that our results would be directly comparable with previously published data (Vela et al., 1995).

RESULTS

Cerebellar morphology in *Rora*$^{sg/sg}$ mice

The characteristic atrophy and dismorphology (undeveloped lobules and altered cyto-architecture) of the cerebellum of the *Rora*$^{sg/sg}$ is shown in Fig.1. In the *Rora*$^{sg/sg}$ mouse (Fig.1A) all the different layers were reduced in size, with a very thin molecular layer and an almost absent granular layer, with Purkinje cells decreased in number and ectopically distributed compared to the wild-type (Fig.1B) (Doulazmi et al., 2001). To quantify the atrophy of the *Rora*$^{sg/sg}$ cerebellum, we evaluated the respective volume of the *Rora*$^{sg/sg}$ and wild-type cerebella (Fig.2A). The estimated volume of the *Rora*$^{sg/sg}$ cerebellum was 2.1 ± 0.04 mm^3 (mean ± SEM) versus 24.5 ± 2.22 mm^3 for the wild-type. These data are consistent with previous work indicating a 10-fold smaller cerebellar mass of the Rorasg/sg mutant compared to the wild-type (F. Frederic et al., unpublished results).

Microglial morphology

Microglial cells and blood vessels were both labeled by NDPase and lectin. Qualitative analysis was performed on sections treated for detection of NDPase activity (Fig.3). This method gives more contrasted pictures than lectin labeling and thus allows a better analysis of cell processes. As shown in Fig. 3A, in wild-type mice, cerebellar microglial cells appeared as faintly stained ramified cells with long thin branched processes as previously described (Perry & Gordon, 1991; Vela et al., 1995). Some rare scattered ellipsoid cells with some thick processes were observed near blood vessels (not shown). In the *Rora*$^{sg/sg}$ cerebellum, microglial cells had strongly stained enlarged cell bodies and a few thick processes. They were mainly located in the vicinity of the remnant molecular layer and near the blood vessels (Fig.3B). By contrast, resting microglial cells were observed in other brain regions of the *Rora*$^{sg/sg}$ mice (not shown).

Quantitative analysis of microglia

As shown in Fig.2B, the estimated microglial cell density in the *Rora*$^{sg/sg}$ cerebellum (22444 ± 5011 cells/mm3) was significantly higher (2.7 fold) than that of the wild-type (8158 ± 1584 cells/mm3) although the *Rora*$^{sg/sg}$ microglial population was 4 fold smaller compared to the wild-type.

DISCUSSION

Our results show that an intense microglial cell reaction occurs specifically in the hypotrophic cerebellum of 30-day old *Rora*$^{sg/sg}$ mice. Significant changes were observed in the morphology of *Rora*$^{sg/sg}$ microglial cells, as well as their number and their density, compared to wild-type littermates. We found that microglial population in the *Rora*$^{sg/sg}$ cerebellum consists exclusively of cells with the morphology characteristic of activated cells. The estimated density of microglial cell in the wild-type is in agreement with an earlier study (Vela et al., 1995), in contrast to the *Rora*$^{sg/sg}$ microglial density which is 2.7 fold higher, due in part to the smaller size of the *Rora*$^{sg/sg}$ cerebellum.

If the atrophic phenomena were equivalent for all cerebellar cell types in *Rora*$^{sg/sg}$, densities of microglial cells in the *Rora*$^{sg/sg}$ and wild-type cerebellum would be equivalent. The higher density of *Rora*$^{sg/sg}$ microglial cells suggests that they have proliferated and/or that some cells committed to disappear have escaped. This implies the action of stimuli that likely are linked to the early neurodegenerative process occurring in the *Rora*$^{sg/sg}$ cerebellum. Round and amoeboid microglia have been shown to populate the mouse developing cerebellum and to expand according to a biphasic kinetic. Throughout late fetal and early postnatal life, numbers of round and amoeboid microglia rise steadily, peak at P7 and rapidly drop. By P10, only resting microglia are found in the cerebellum (Ashwell, 1990). Round and amoeboid microglia are concerned with phagocytosis to clear the developing cerebellum from additional dying neurons and axons likely to be inappropriately connected. In the *Rora*$^{sg/sg}$ cerebellum, degeneration of neuronal cells begins with the death of Purkinje cells between P0 and P5 and develops during the first month of life (Herrup & Mullen, 1979; Vogel et al., 2000). It completely overlaps the postnatal growth phase of round and amoeboid microglia and the short period during which microglial population shifts from activated to resting cells. Neurodegenerative cell death might prolong the presence of phagocytic microglia in the *Rora*$^{sg/sg}$ cerebellum until degenerating neurons are cleared, either by increasing the lifespan of microglial cell or by inducing them to proliferate. Moreover, the presence of microglial cells which are already differentiated into phagocytic cells in the degenerating area may explain the significant decrease (approximatively 40%) as early as P5 in the volume of the *Rora*$^{sg/sg}$ cerebellum compared to controls (Vogel et al., 2000).

CNS inflammation is characterised by glial cell (microglia, astrocyte and oligodendrocyte) activation, glial cell proliferation and de novo synthesis of cytokines. The presence of astriogliosis in the staggerer cerebellum was described twenty years ago (Seyfried & Yu, 1984; Levine et al., 1986). We have previously shown elevated levels of pro-inflammatory cytokines (IL-1ß and IL-6) in the cerebellum of one-month-old Rorasg/sg mice (Lemaigre-Dubreuil et al., 1996; Vernet-der Garabedian et al., 1998). We described here an activated and hyperplasic microglial cell population in the Rorasg/sg cerebellum. Taken together, these data indicate that a typical inflammatory process develops early in the $Rora^{sg/sg}$ cerebellum in reponse to the massive neuron loss and that it is still active one month after the beginning of the inflammatory phenomenon.

ACKNOWLEDGMENTS

This work was supported by Europeen Community (TMR Neuril no. FMRX CT97-0149 and Biomed Cybrainet no. CT97-2492 to J.M.). NJ was supported by fellowships from the association France-Alzheimer. We thank Dr. A Lohof for critical reading of the manuscript and P. Bouquet for excellent technical assistance in histology.

Figure legends:

Fig.1 : Cerebella from one month old homozygous *Rora*$^{sg/sg}$ (A) and wild-type mice (B). Midsagittal sections were stained with cresyl violet. The lobulation and the trilaminar organization of the cerebellar cortex as shown in the wild-type cerebellum (B) are much reduced in the *Rora*$^{sg/sg}$ cerebellum (A). Note the significant atrophy of the *Rora*$^{sg/sg}$ cerebellum compared to the wild-type.

Fig.2 : Quantification of cerebellar volumes of wild-type and *Rora*$^{sg/sg}$ mice (A) and of microglial cell densities in wild-type and *Rora*$^{sg/sg}$ cerebella (B). Volumes of cerebella were determined as described in Materials and Methods. Microglia were identified with lectin labeling. Error bars indicate SEM.

Fig.3 : Morphology of microglial cells, revealed using the NDPase activity method, in wild-type (A) and *Rora*$^{sg/sg}$ (B) cerebella. Resting microglia cells (small cell body and long branched thin processes) in the cerebellum of the wild-type are indicated by arrow-heads; they contrast with the appearance of activated *Rora*$^{sg/sg}$ microglia, characterized by an enlarged strongly stained cell body and short thick processes (arrow-heads). BV and thin arrow indicate labeling of blood vessels.

REFERENCES

Ashwell, K. (1990). Microglia and cell death in the developing mouse cerebellum. Developmental Brain Reseach. **55**, 219-230.

Basu, A., Krady J.K. and S.W., L. (2004). Interleukin-1 : A Master Regulator of Neuroinflammation. J. Neurosc. Research. **78**, 151-156.

Doulazmi, M., Frederic, F., Capone, F., Becker-Andre, M., Delhaye-Bouchaud, N. and Mariani, J. (2001). A comparative study of Purkinje cells in two RORalpha gene mutant mice: staggerer and RORalpha(-/-). Brain Res Dev Brain Res. **127**, 165-74.

Doulazmi, M., Frederic, F., Lemaigre-Dubreuil, Y., Hadj-Sahraoui, N., Delhaye-Bouchaud, N. and Mariani, J. (1999). Cerebellar Purkinje cell loss during life span of the heterozygous staggerer mouse (Rora(+)/Rora(sg)) is gender-related. J Comp Neurol. **411**, 267-73.

Hamilton, B.A., Frankel, W.N., Kerrebrock, A.W., Hawkins, T.L., FitzHugh, W., Kusumi, K., Russell, L.B., Mueller, K.L., van Berkel, V., Birren, B.W., Kruglyak, L. and Lander, E.S. (1996). Disruption of the nuclear hormone receptor RORalpha in staggerer mice [published erratum appears in Nature 1996 May 23;381(6580):346]. Nature. **379**, 736-9.

Herrup, K. and Mullen, R.J. (1979). Regional variation and absence of large neurons in the cerebellum of the staggerer mouse. Brain Res. **172**, 1-12.

Herrup, K. and Mullen, R.J. (1979). Staggerer chimeras: intrinsic nature of Purkinje cell defects and implications for normal cerebellar development. Brain Res. **178**, 443-57.

Jarvis, C.I., Staels, B., Brugg, B., Lemaigre-Dubreuil, Y., Tedgui, A. and Mariani, J. (2002). Age-related phenotypes in the staggerer mouse expand the RORalpha nuclear receptor's role beyond the cerebellum. Mol Cell Endocrinol. **186**, 1-5.

Kreutzberg, G.W. (1996). Microglia: a sensor for pathological events in the CNS. Trends Neurosci. **19**, 312-8.

Lemaigre-Dubreuil, Y., Brugg, B., Chianale, C., Delhaye-Bouchaud, N. and Mariani, J. (1996). Over-expression of interleukin-1beta-converting enzyme mRNA in staggerer cerebellum. Neuroreport. **7**, 1777-1780.

Levine, S.M., Seyfried, T.N., Yu, R.K. and Goldman, J.E. (1986). Immunocytochemical localisation of GD3 ganglioside to astrocytes in murine cerebellar mutants. Brain Res. **374**, 260-269.

Matsui, T., Sashihara, S., Oh, Y. and Waxman, S.G. (1995). An orphan nuclear receptor, mROR alpha, and its spatial expression in adult mouse brain. Brain Res Mol Brain Res. **33**, 217-26.

Monnier, Z., Bahjaoui-Bouhaddi, M., Bride, J., Bride, M., Math, F. and Propper, A. (1999). Structural and immunohistological modifications in olfactory bulb of the *staggerer* mutant mouse. Biol. Cell. **91**, 29-44.

Murabe, Y. and Sano, Y. (1982). Morphological studies on neuroglia. VI. Postnatal development of microglial cells. Cell Tissue Res. **225**, 469-485.

Perry, V.H. and Gordon, S. (1991). Macrophages and the nervous system. Intern. Rev. Cytol. **125**, 203-244.

Seyfried, T.N. and Yu, R.K. (1984). Cellular localization of gangliosides in the mouse cerebellum: analysis using neurological mutants. Adv. Exp. Med. Biol. **174**, 169-81.

Shojaeian, H., Herrup, K., Guastavino, J.M., Delhaye-Bouchaud, N. and Mariani, J. (1994). Development studies of the inferior olivary nucleus in staggerer mutant mice. Dev.Brain Res. **82**, 18-28.

Sidman, R.L., Lane, P.W. and Dickie, M.N. (1962). *staggerer*, a new mutation in the mouse affecting the cerebellum. Science. **137**, 610-612.

Streit, W.J. and Kreutzberg, G.W. (1987). Lectin binding by resting and reactive microglia. J. Neurocytol. **16**, 249-260.

Vela, J.M., Dalmau, I., Gonzalez, B. and Castellano, B. (1995). Morphology and Distribution of Microglial Cells in the Young and Adult Mouse Cerebellum. J. Comp. Neurol. **361**, 602-616.

Vernet-der Garabedian, B., Lemaigre-Dubreuil, Y., Delhaye-Bouchaud, N. and Mariani, J. (1998). Abnormal IL-1ß cytokine expression in the cerebellum of the ataxic mutant mice *staggerer* and *Lurcher*. Molec. Brain Res. **62**, 224-227.

Vogel, M.W., Sinclair, M., Qiu, D. and Fan, H. (2000). Purkinje cell fate in staggerer mutants : agenesis versus cell death. Neurobiol. **42**, 323-337.

Wirenfeldt, M., Dalmau, I. and Finsen, B. (2003). Estimation of Absolute Microglial Cell Numbers in Mouse Fascia Dentata Using Unbiased and Efficient Stereological Cell Counting Principles. Glia. **44**, 129-139.

Wu, C.H., Wen, C.Y., Shieh, J.Y. and Ling, E.A. (1992). A quantitative and morphometric study of the transformation of amoeboid microglia into ramified microglia in the developing corpus callosum in rats. J. Anat. **181**, 423-430.

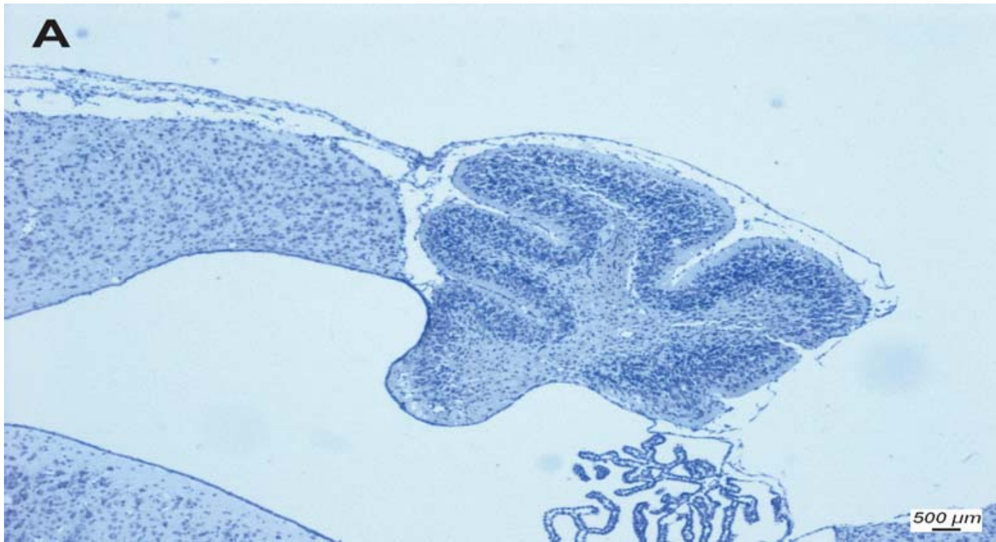
A
500 µm

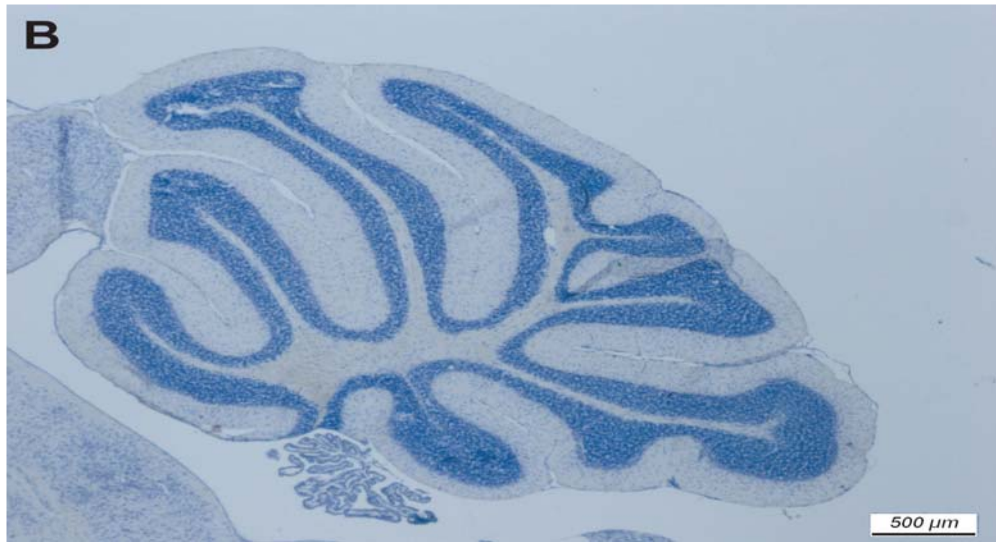
B
500 µm

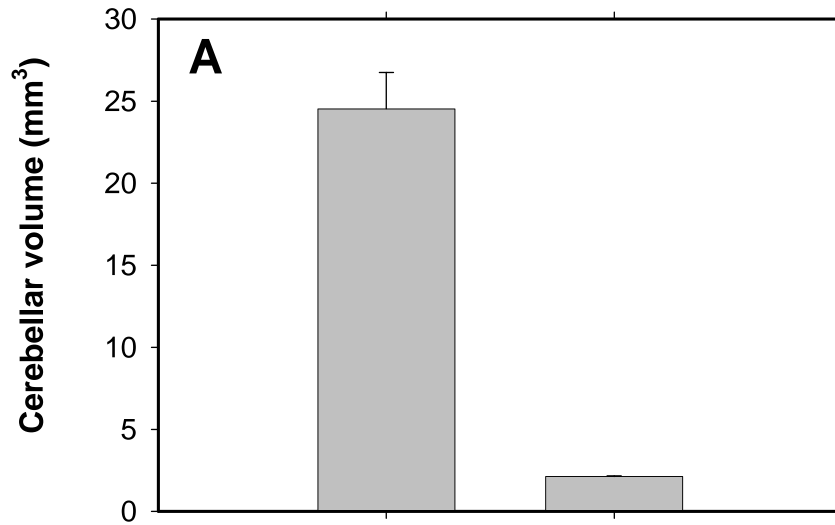
A
Cerebellar volume (mm^3)
30
25
20
15
10
5
0

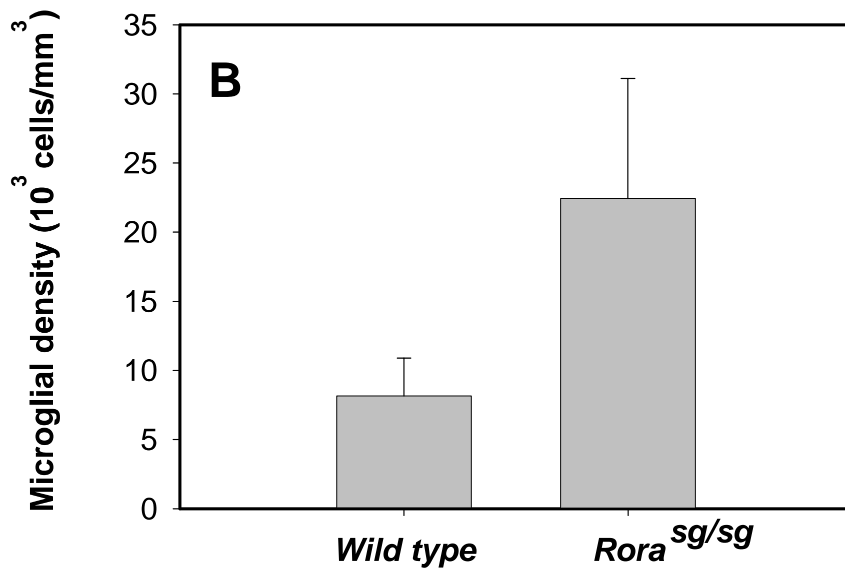
B
Microglial density (10^3 cells/mm^3)
35
30
25
20
15
10
5
0
Wild type
Rora$^{sg/sg}$

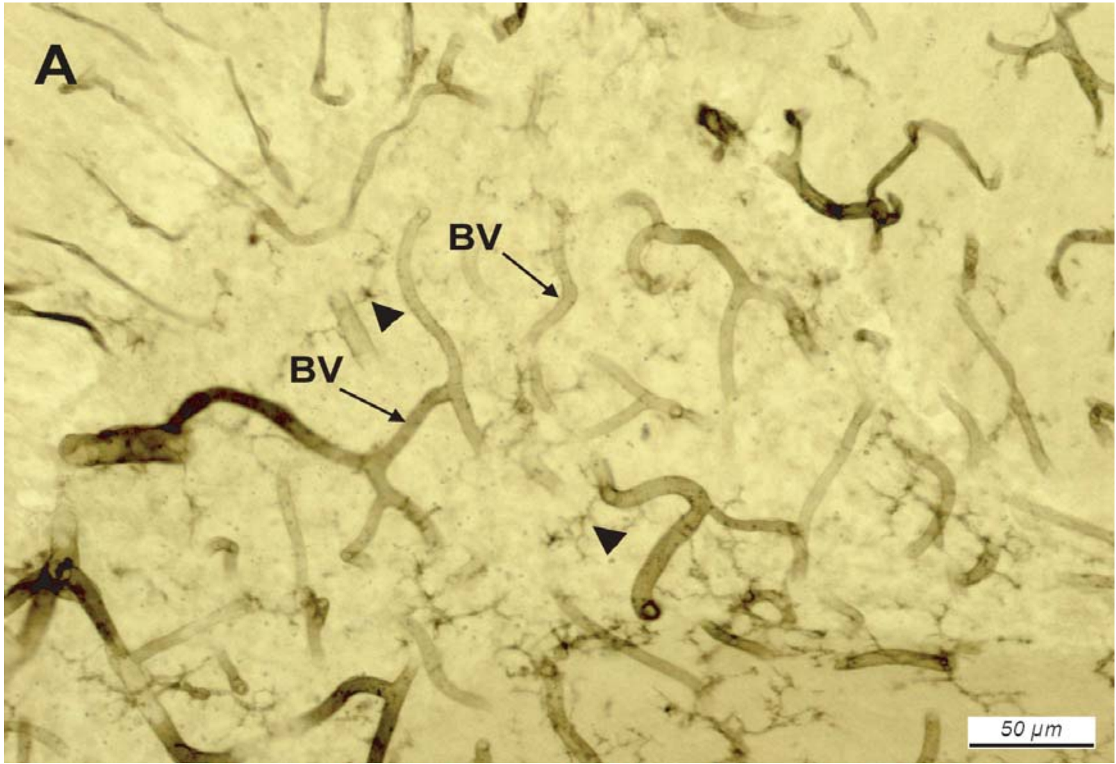
A
BV
BV
50 μm

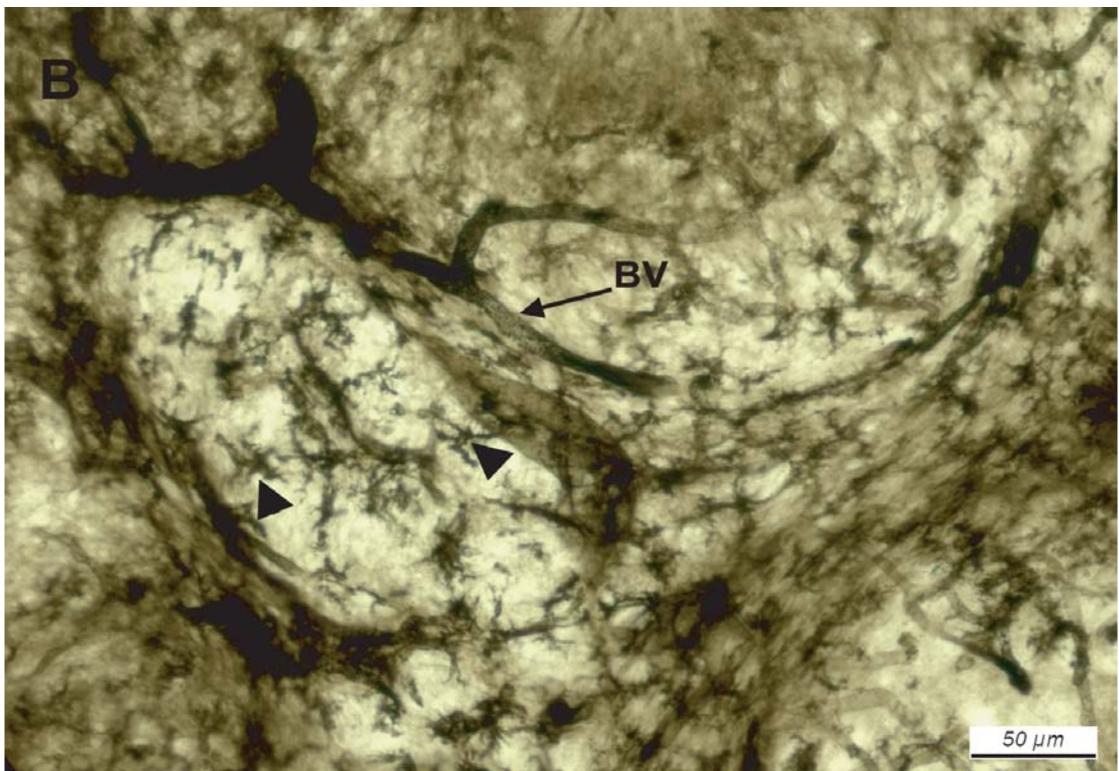
B
BV
50 μm